

Time-dependent variational Monte Carlo study of the dynamic structure factor for bosons in an optical lattice

Mathias Gartner,¹ Ferran Mazzanti,² and Robert E. Zillich¹

¹*Institute for Theoretical Physics, Johannes Kepler University Linz, Altenberger Straße 69, 4040 Linz, Austria*

²*Departament de Física i Enginyeria Nuclear, Campus Nord B4-B5, Universitat Politècnica de Catalunya, E-08034 Barcelona, Spain*

(Dated: February 16, 2022)

We study the dynamics of a one-dimensional Bose gas at unit filling in both shallow and deep optical lattices and obtain the dynamic structure factor $S(k, \omega)$ by monitoring the linear response to a weak probe pulse. In order to do that we introduce a new procedure, based on the time-dependent variational Monte Carlo method (tVMC), which allows to evolve the system in real time, using as a variational model a Jastrow-Feenberg wave function that includes pair correlations. Comparison with exact diagonalization results of $S(k, \omega)$ obtained on a lattice in the Bose-Hubbard limit shows good agreement of the dispersion relation for sufficiently deep optical lattices, while for shallow lattices we observe the influence of higher Bloch bands. We also investigate non-linear response and obtain the excitation spectrum, albeit broadened, by higher harmonic generation after a strong pulse with a single low wave number. As a remarkable feature of our simulations we demonstrate that the full excitation spectrum can be retrieved from the stochastic noise inherent in any Monte Carlo method, without applying an actual perturbation.

The dynamic structure factor $S(k, \omega)$ is a fundamental quantity as it contains the maximal information about the dynamics of many-body quantum systems that one can obtain by inelastic scattering [1], such as the excitation energies $\omega(k)$ and the lifetime of collective excitations. In quantum gases $S(k, \omega)$ can be measured by Bragg spectroscopy [2], with relative momentum and energy resolution similar to inelastic neutron scattering in condensed matter [3]. The calculation of $S(k, \omega)$ is a demanding task beyond very simple Hamiltonians or approximations, such as the Bijl-Feynman model [4, 5], or the Bogoliubov-de Gennes technique in the mean field limit [6, 7]. Advanced variational methods based on action minimization, such as the correlated basis function approach [8] or the multi-configuration time-dependent Hartree algorithm [9], can achieve much more accurate results. All these methods are reliable in many cases but are not expected to work well in all situations. Monte Carlo methods, on the other hand, are known to be able to produce statistically exact predictions for bosons, although this only applies to the ground state at zero temperature [10], or to static ensemble averages at finite temperature [11]. Access to the excitation spectrum is restricted to the evaluation of the dynamic response in imaginary time and its reconstruction in frequency space by inverting the Laplace transform. This is a rather difficult procedure as Laplace inversion is a well known ill-posed mathematical problem, worsened in practice by the fact that the stochastic noise of the simulation is exponentially amplified in the result. The way to tackle these problems is to build many reconstructions of the response and to use stochastic methods based on simulated annealing [12] or genetic algorithms [13, 14] to produce an approximate dynamic structure factor. While this method can yield good results, it is computationally

very expensive and usually gets only the broad features, not resolving well the fine details of the response. Other methods available for dynamic simulations are either restricted to lattice systems, like time-evolving block decimation [15], nonequilibrium dynamical mean-field theory [16], and the time-dependent density matrix renormalization group method [17–19], or they work best in one dimension, like methods based on continuous matrix product states [20]. Consequently, accurate methods that allow for time dependent simulations of strongly correlated many-body systems which can describe the linear, but also nonlinear response to perturbations, are in demand.

The time-dependent variational Monte Carlo (tVMC) method [21–23] is particularly suitable for the study of quantum many-body dynamics, allowing for perturbations of any strength. It can be applied to analyze many different situations, such as ramping up the lattice depth [24] or interaction quenches [22], as well as many-body dynamics far from equilibrium [25]. It has also been extended to wave functions based on artificial neural networks [26, 27]. In this work we present a new way to calculate the dynamic structure factor $S(k, \omega)$ of strongly interacting bosons in continuous space, based on tVMC. We use it to analyze the dynamic response of a Bose gas in an optical lattice in one dimension. We study the response to an external perturbation $\delta V_p(x, t)$, and monitor the density fluctuations $\delta \rho(x, t)$ during the time evolution. In the linear response regime, the ratio of their Fourier transforms is the density response function, with its imaginary part being the dynamic structure factor [28]. We perform a series of simulations for a system of N identical bosons of mass m , moving in a one dimensional optical lattice characterized by an external potential $V(x) = V_0 \sin^2(k_L x)$ and interacting via a con-

tact potential. The Hamiltonian reads

$$H = \sum_{i=1}^N \left(-\frac{\partial^2}{\partial x_i^2} + V(x_i) + \delta V_p(x_i, t) \right) + g \sum_{i<j}^N \delta(x_i - x_j), \quad (1)$$

with the coupling constant g parametrizing the strength of the two-body interaction. Throughout this work, energies are given in units of the recoil energy $E_r = \hbar^2 k_L^2 / 2m$, and we use $x_0 = \pi/k_L$ and $t_0 = \hbar/E_r$ as length and time unit, respectively.

In the deep lattice limit where the amplitude V_0 is large, H can be approximated by the lattice Hamiltonian of the single-band Bose-Hubbard model (BHM) [29, 30] $H_{\text{BHM}} = -J \sum_{i<j}^N b_i^\dagger b_j + U/2 \sum_i^N n_i(n_i - 1)$, where b_i^\dagger , b_i and n_i are the creation, annihilation and number operator for bosons at lattice site i . For given V_0 and g in Eq. (1), the on-site interaction U and the hopping parameter J of the BHM can be evaluated numerically performing band-structure calculations [31]. Within our continuous space tVMC simulations, we can access both the BHM regime and the region of shallow optical lattices, where the single-band BHM model is no longer valid.

The tVMC method relies on a model wave function with variational parameters that are propagated in time. For modeling the time-dependent wavefunction $\Phi(\mathbf{x}, t)$ of the many-body system, with $\mathbf{x} = (x_1, \dots, x_N)$, we use a Jastrow-Feenberg ansatz [32] with one- and two-particle correlation functions

$$\Phi(\mathbf{x}, t) = \prod_i^N f_1(x_i, t) \prod_{i,j}^N f_2(x_i - x_j, t). \quad (2)$$

The effect of the contact interaction in the Hamiltonian (1) can be directly incorporated in the wavefunction by using an appropriate boundary condition on f_2 for $x_i = x_j$, according to [33]. The correlation functions f_1 and f_2 depend on time-dependent complex variational parameters $\alpha_m(t) = \{\alpha_{m1}(t), \alpha_{m2}(t), \dots, \alpha_{mP_m}(t)\}$ with $m = 1, 2$. We thus can write (2) as

$$\Phi(\mathbf{x}, \alpha(t)) = \prod_m \exp \left(\sum_{p=1}^{P_m} \mathcal{O}_{mp}(\mathbf{x}) \alpha_{mp}(t) \right), \quad (3)$$

where every parameter α_{mp} is coupled to a local operator $\mathcal{O}_{mp}(\mathbf{x})$, specified further below. In the following, we abbreviate $K \equiv (m, p)$. As shown in [21], the equations governing the time evolution of the variational parameters are

$$i \sum_{K'} S_{KK'} \dot{\alpha}_{K'} = \langle \mathcal{E} \mathcal{O}_K \rangle - \langle \mathcal{E} \rangle \langle \mathcal{O}_K \rangle, \quad (4)$$

with $S_{KK'} = \langle \mathcal{O}_K \mathcal{O}_{K'} \rangle - \langle \mathcal{O}_K \rangle \langle \mathcal{O}_{K'} \rangle$ and the local energy $\mathcal{E} = \frac{\langle \Phi | H | \Phi \rangle}{\langle \Phi | \Phi \rangle}$. These coupled ordinary differential equations can be solved numerically, where in every

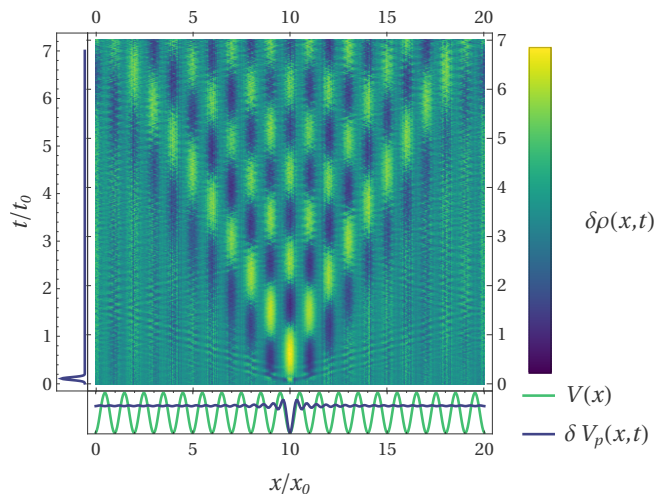


FIG. 1. Sketch of the real time simulation used to obtain the dynamic structure factor. Initially the system is in the ground state (obtained via i-tVMC) of the optical potential $V(x)$ (green line). At time $t = 0$, a pulsed perturbation $\delta V_p(x, t)$ with a Gaussian time profile (blue line on the left) and a superposition of various momentum modes $\sum_j \sin^2(k_j x)$ (blue line at the bottom) is turned on. The main color map shows the propagation in time and space of the density fluctuation $\delta \rho = \rho(x, t) - \rho(x, 0)$ induced by the perturbation. The amplitude of the pulse δV_p is magnified by a factor of 20 in this sketch.

timestep the expectation values forming the coefficient matrix $S_{KK'}$ and the right hand side of the equation system are calculated by Monte Carlo integration.

We use very generic one- and two-particle correlation functions f_1 and f_2 represented by a linear combination of third order B-splines [34] as the \mathcal{O}_K operators in the wavefunction (3). These are piecewise polynomial functions, restricted locally to certain intervals Y_p centered at the points of a uniform grid. For each interval Y_p we denote the corresponding spline by $B_p(x)$ and define $\mathcal{O}_{1p}(\mathbf{x}) = \sum_i B_p(x_i)$ and $\mathcal{O}_{2p}(\mathbf{x}) = \sum_{i<j} B_p(|x_i - x_j|)$ as the local operators for the one- and two-body correlation functions, respectively, which allows us to write the trial wavefunction in the convenient form of Eq. (3). In all the simulations presented in this work we use 400 ($P_1 = P_2 = 200$) complex variational parameters α_K . We have checked that these values produce converged results for the problem addressed in this work.

For the calculations we proceed as follows: we first perform tVMC simulations in imaginary time (i-tVMC) with $\delta V_p = 0$ to obtain the ground state of the Hamiltonian in Eq. (1). The result is then used as the initial wavefunction for the real time simulation, with the perturbing potential δV_p turned on. By monitoring the density fluctuations $\delta \rho(x, t)$ (see Fig. 1) we can use linear response theory [28] to estimate the dynamic struc-

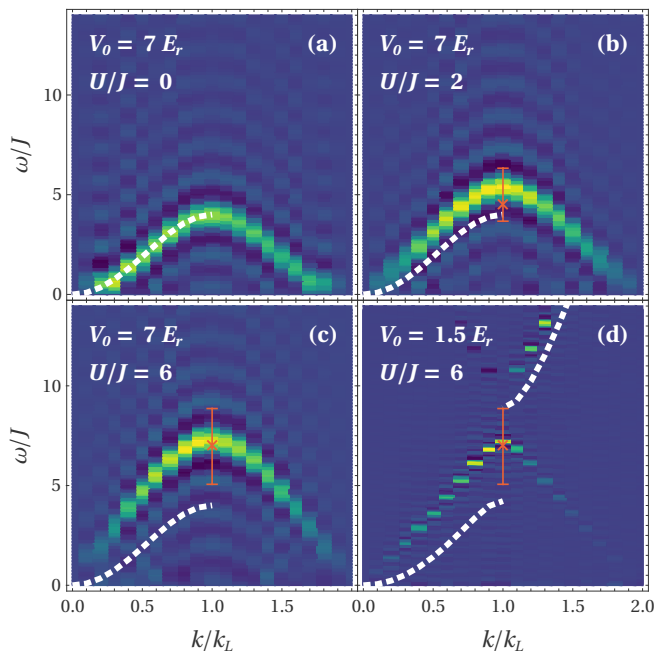


FIG. 2. Dynamic structure factor $S(k, \omega)$ from tVMC simulations for a system with optical potential strength $V_0 = 7 E_r$ and equivalent BHM parameter $U/J = 0; 2; 6$ (panels (a)–(c)), and $V_0 = 1.5 E_r$ with $U/J = 6$ (panel (d)). The dashed white lines show the dispersion of non-interacting particles ($U = 0$) for the given value of V_0 , obtained from band structure calculations. The red bar indicates the width of the excitation band of $S(k, \omega)$ of Ref. [35].

ture factor $S(k, \omega) = -\frac{1}{\pi} \text{Im} \left[\delta \tilde{\rho}(k, \omega) / \delta \tilde{V}_p(k, \omega) \right]$, where $\delta \tilde{\rho}(k, \omega)$ and $\delta \tilde{V}_p(k, \omega)$ are the space and time Fourier transforms of the density and the perturbing potential, respectively.

We calculate the dynamic structure factor $S(k, \omega)$ for several values of the coupling strength g and the optical lattice amplitude V_0 . We use $N = 20$ particles with a density $n = 1/x_0$ in a simulation box of size $L = x_0 N$ with periodic boundary conditions, corresponding to unit filling. To excite the system we apply a multi-mode pulse with a Gaussian time profile

$$\delta V_p(x, t) = V_e e^{-(t-t_e)^2/\tau^2} \sum_j^{j_{\max}} \sin^2(k_j x), \quad (5)$$

where the spatial part is a superposition of up to $j_{\max} = 40$ modes with wave numbers $k_j = 2\pi j/L$. In particular, we choose $V_e = 0.0125 E_r$, $t_e = 0.1 t_0$ and $\tau = 0.04 t_0$, which only changes the ground state energy by less than 0.25%, so as to guarantee that the perturbation is weak enough for linear response theory to apply. In the linear regime we can get the full excitation spectrum in a single tVMC simulation since modes are excited simultaneously, but independently of each other. The short pulse length τ also ensures that it excites a

broad range $2\pi/\tau$ of energies. In any case, the pulse in Eq. (5) can be easily tailored, to excite only selected modes if required.

We present in Fig. 2 the dynamic structure factor $S(k, \omega)$ in units of k_L and J . Panels (a)–(c) show $S(k, \omega)$ for a deep optical potential $V_0 = 7 E_r$ and interaction strengths $g = 0; 0.14; 0.41 E_r/k_L$, corresponding to the ratios $U/J = 0; 2; 6$ of the BHM, respectively. Panel (d) shows $S(k, \omega)$ for a shallow lattice with $V_0 = 1.5 E_r$ and $g = 2.8 E_r/k_L$, associated to the equivalent BHM ratio $U/J = 6$. White dashed lines denote the Bloch dispersion of non-interacting particles. The tVMC result for $U/J = 0$ in panel (a) demonstrates that the peaks in $S(k, \omega)$ reproduce the exact non-interacting Bloch dispersion perfectly. The broadening of the tVMC dispersion, as well as the ringing oscillations, are artifacts resulting from the Fourier transform over a finite simulation time window of length $T = 10 t_0$. As U/J is increased, the excitation energies increase also, and the dispersion becomes linear for small k . The positions of the peaks in $S(k, \omega)$ are in good agreement with results of [35] obtained by exact diagonalization of the BHM (see the red bar and central position in panels (b) to (d)). The shape of $S(k, \omega)$, however, differs somewhat from the results in [35], where a more complex structure was obtained for $N = 16$. The red bars in Fig. 2 represent this broadening, with the red cross in the middle indicating the position, of the main peak. For the shallow optical lattice case shown in panel (d), corresponding to $V_0 = 1.5 E_r$, the band gap is comparable with the band width. In such a case the single-band BHM would not be applicable. The dispersion is linear over a wider range of k values than in the deep lattice, while the maximum of the first band hardly changes. In such a shallow lattice, we also observe an energy increase of the second band with respect to the Bloch dispersion. Notice that the seemingly smaller broadening of the curve in panel (d) is due to the fact that all energies are expressed in units of J , which is $J = 0.04 E_r$ for $V_0 = 7 E_r$ and $J = 0.16 E_r$ for $V_0 = 1.5 E_r$.

In fact, the tVMC method is not restricted to weak perturbations, and thus one can use it to explore the response of the system outside the linear regime. In order to demonstrate this, we again perturb the same Bose system at unit filling in the optical lattice with $V_0 = 3 E_r$ and $U/J = 6$, but this time with a strong pulse. Instead of exciting all wave numbers simultaneously with the weak pulse in Eq. (5), we excite only the lowest mode compatible with the periodic boundary condition, with wave number $k_1 = 2\pi/L = 0.1 k_L$, but with a pulse strength equal to the amplitude of the lattice potential, $V_e = V_0$. We use a pulse length τ five time longer than in the linear response simulations previously described, and also set $t_e = 0.5 t_0$ to move the peak of the pulse to larger times for a smooth switch-on of the perturbation. Overall, the integrated pulse strength is 30 times

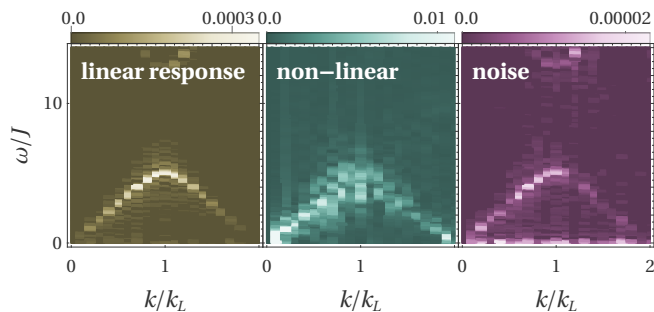


FIG. 3. Fourier transformation $|\delta\tilde{\rho}(k, \omega)|$ of the density fluctuations obtained with three different tVMC simulation variants. The left panel shows the response to a weak multi-mode pulse of the form given in Eq. (5). In the central panel, the system is excited with a single mode at $k = 0.1 k_L$ with an amplitude as large as the lattice potential ($V_e = V_0$). On the right, no perturbation is applied and the density fluctuations in the time propagation are solely due to the stochastic noise in the Monte Carlo simulation. The system parameters used in these simulation are $U = 6J$ and $V_0 = 3E_r$. Note that the scales are different for the three simulations.

stronger than that of the weak multi-mode pulse to compare with. Since outside the linear regime $S(k, \omega)$ no longer describes the full response of the system to the perturbation, we directly show $|\delta\tilde{\rho}(k, \omega)|$. The central panel of Fig. 3 shows $|\delta\tilde{\rho}(k, \omega)|$ after the strong pulse with wave number k_1 . As it could be expected, a very pronounced peak in the non-linear response appears at k_1 . However, the strong pulse excites a wide range of multiples of k_1 via higher harmonic generation. For comparison, in the left panel of Fig. 3 we show $|\delta\tilde{\rho}(k, \omega)|$ for the weak multi-mode pulse $\delta V_p(x, t)$, Eq. (5). Note that in the linear response regime $|\delta\tilde{\rho}(k, \omega)|$ conveys the same information as $S(k, \omega)$, see the previous Fig. 2. Compared to the linear response to the weak multi-mode pulse, the non-linear response exhibits a much broader excitation band, but it still follows the dispersion relation obtained from linear response; the broadening is expected for higher harmonic generation in a system with a non-linear dispersion. A sufficiently strong long wavelength perturbation yields the full excitation spectrum, albeit with significant broadening.

An even more remarkable feature of the tVMC method is that the full excitation spectrum can also be obtained in the opposite limit, i.e. applying no perturbation at all. We can simply propagate the ground state in real time, and the stochastic noise, inherent to any Monte Carlo method, produces fluctuations around the exact time evolution. The Monte Carlo noise has non-zero projection over all excited states, and so we can use it to calculate the excitation spectrum of all modes. Since there is no explicit perturbation $\delta\tilde{V}_p(k, \omega)$ in this approach – and therefore linear response theory can not be applied directly – we report again $|\delta\rho(k, \omega)|$, shown in the right panel of Fig. 3. This spectrum, generated entirely by

the stochastic noise, is nearly identical to the linear response result shown in the left panel. In this way, the Monte Carlo noise can be effectively used to explore the excitation spectrum of the system, although as seen from the color scales in Fig. 3 the noise generated spectrum is much weaker. As expected, the noise is reduced when increasing the sample size per time step, but the signal-to-noise ratio of the density fluctuation power spectrum remains unchanged.

Our result suggests a new simulation strategy of propagating the unperturbed ground state in time, rather than exciting the specific modes with suitable temporally and spatially shaped weak or strong external pulses. With this new type of simulation we can for example determine the excitation spectrum in a large range of ω - and k -values, which is useful when analyzing a new system with little knowledge about the relevant range of energies and momenta to explore. It has the added benefit of not having to choose any specific form for the perturbation potential.

In summary, we have explored the possibility of using time-dependent variational Monte Carlo (tVMC) to obtain the dynamic structure function $S(k, \omega)$, or more generally the excitation spectrum, of many-body quantum systems under the action of a weak, pulsed multi-mode perturbation. Specifically, we have analyzed the linear and nonlinear dynamics of a one-dimensional system of bosons in an optical lattice described by a continuous Hamiltonian. In both deep and shallow lattices, we explore several interaction strengths corresponding to the same ratio U/J of the Hubbard interaction and hopping parameters, to assess the universality of the dependence of the excitation spectrum on it. For shallow lattices and as expected, we observe a deviation from the single-band Bose-Hubbard result, with the dispersion being linear over a wider range of momenta. However, for the lowest band, the excitation energy at the edge of the Brillouin zone is remarkably universal.

Besides the weak perturbation regime where linear response theory applies, we have also explored the dynamics after a very strong perturbation, and the dynamics with no perturbation at all. In the latter case we simply propagate the optimized ground state in real time to obtain the excitation spectrum from the fluctuations due to the stochastic noise intrinsic to every Monte Carlo method. This can be useful when studying complex systems where the exact nature of the excitations is hard to discern, and the right choice of the perturbation and response operators is not so obvious. In order to explore the non-linear regime, we apply pulses coupling to a single mode, but with peak strengths of the order of the optical lattice depth itself. These strong pulses excite the full range of wave numbers via higher harmonic generation. This is relevant for Bragg spectroscopy of the excitation spectrum, since only one or few momentum transfers need to be chosen to obtain an approximate

$S(k, \omega)$ for a wide range of momenta.

M.G. and R.E.Z thank G. Carleo and M. Holzmann for fruitful discussions and acknowledge computational resources of the Scientific Computing Administration at Johannes Kepler University. F.M. acknowledges financial support by grant PID2020-113565GB-C21 funded by MCIN/AEI/10.13039/501100011033, and from Secretaria d'Universitats i Recerca del Departament d'Empresa i Coneixement de la Generalitat de Catalunya, co-funded by the European Union Regional Development Fund within the ERDF Operational Program of Catalunya (project QuantumCat, ref. 001-P-001644).

-
- [1] R. G. Newton, *Scattering Theory of Waves and Particles* (Courier Corporation, 2002).
- [2] J. Stenger, S. Inouye, A. P. Chikkatur, D. M. Stamper-Kurn, D. E. Pritchard, and W. Ketterle, Bragg Spectroscopy of a Bose-Einstein Condensate, *Phys. Rev. Lett.* **82**, 4569 (1999).
- [3] L. Sobirey, N. Luick, M. Bohlen, H. Biss, H. Moritz, and T. Lompe, Observation of superfluidity in a strongly correlated two-dimensional Fermi gas, *Science* **372**, 844 (2021).
- [4] A. Bijl, The lowest wave function of the symmetrical many particles system, *Physica* **7**, 869 (1940).
- [5] R. P. Feynman and M. Cohen, Energy Spectrum of the Excitations in Liquid Helium, *Phys. Rev.* **102**, 1189 (1956).
- [6] L. Pitaevskii and S. Stringari, *Bose-Einstein Condensation and Superfluidity*, International Series of Monographs on Physics (Oxford University Press, 2016).
- [7] F. Dalfovo, S. Giorgini, L. P. Pitaevskii, and S. Stringari, Theory of Bose-Einstein condensation in trapped gases, *Rev. Mod. Phys.* **71**, 463 (1999).
- [8] C. E. Campbell, E. Krotscheck, and T. Lichtenegger, Dynamic many-body theory: Multiparticle fluctuations and the dynamic structure of ^4He , *Phys. Rev. B* **91**, 184510 (2015).
- [9] A. U. J. Lode, C. Lévêque, L. B. Madsen, A. I. Streltsov, and O. E. Alon, Colloquium: Multiconfigurational time-dependent Hartree approaches for indistinguishable particles, *Rev. Mod. Phys.* **92**, 011001 (2020).
- [10] I. Kosztin, B. Faber, and K. Schulten, Introduction to the Diffusion Monte Carlo Method, *American Journal of Physics* **64**, 633 (1996).
- [11] D. M. Ceperley, Path integrals in the theory of condensed helium, *Rev. Mod. Phys.* **67**, 279 (1995).
- [12] R. Rota, J. Casulleras, F. Mazzanti, and J. Boronat, Quantum Monte Carlo estimation of complex-time correlations for the study of the ground-state dynamic structure function, *J. Chem. Phys.* **142**, 114114 (2015).
- [13] E. Vitali, M. Rossi, L. Reatto, and D. E. Galli, Ab initio low-energy dynamics of superfluid and solid ^4He , *Phys. Rev. B* **82**, 174510 (2010).
- [14] G. Bertaina, M. Motta, M. Rossi, E. Vitali, and D. E. Galli, One-Dimensional Liquid ^4He : Dynamical Properties beyond Luttinger-Liquid Theory, *Phys. Rev. Lett.* **116**, 135302 (2016).
- [15] G. Vidal, Efficient Simulation of One-Dimensional Quantum Many-Body Systems, *Phys. Rev. Lett.* **93**, 040502 (2004).
- [16] H. Aoki, N. Tsuji, M. Eckstein, M. Kollar, T. Oka, and P. Werner, Nonequilibrium dynamical mean-field theory and its applications, *Rev. Mod. Phys.* **86**, 779 (2014).
- [17] S. R. White, Density matrix formulation for quantum renormalization groups, *Phys. Rev. Lett.* **69**, 2863 (1992).
- [18] A. E. Feiguin and S. R. White, Time-step targeting methods for real-time dynamics using the density matrix renormalization group, *Phys. Rev. B* **72**, 020404 (2005).
- [19] U. Schollwöck, The density-matrix renormalization group, *Rev. Mod. Phys.* **77**, 259 (2005).
- [20] F. Verstraete and J. I. Cirac, Continuous Matrix Product States for Quantum Fields, *Phys. Rev. Lett.* **104**, 190405 (2010).
- [21] G. Carleo, F. Becca, M. Schiró, and M. Fabrizio, Localization and Glassy Dynamics Of Many-Body Quantum Systems, *Sci. Rep.* **2**, 243 (2012).
- [22] G. Carleo, F. Becca, L. Sanchez-Palencia, S. Sorella, and M. Fabrizio, Light-cone effect and supersonic correlations in one- and two-dimensional bosonic superfluids, *Phys. Rev. A* **89**, 031602 (2014).
- [23] G. Carleo, L. Cevolani, L. Sanchez-Palencia, and M. Holzmann, Unitary Dynamics of Strongly Interacting Bose Gases with the Time-Dependent Variational Monte Carlo Method in Continuous Space, *Phys. Rev. X* **7**, 031026 (2017).
- [24] B. Gardas, J. Dziarmaga, and W. H. Zurek, Dynamics of the quantum phase transition in the one-dimensional Bose-Hubbard model: Excitations and correlations induced by a quench, *Phys. Rev. B* **95**, 104306 (2017).
- [25] J. Eisert, M. Friesdorf, and C. Gogolin, Quantum many-body systems out of equilibrium, *Nature Phys* **11**, 124 (2015).
- [26] G. Carleo and M. Troyer, Solving the quantum many-body problem with artificial neural networks, *Science* **355**, 602 (2017).
- [27] M. Schmitt and M. Heyl, Quantum Many-Body Dynamics in Two Dimensions with Artificial Neural Networks, *Phys. Rev. Lett.* **125**, 100503 (2020).
- [28] D. Pines and P. Nozières, *The Theory of Quantum Liquids: Normal Fermi Liquids* (W.A. Benjamin, 1966).
- [29] J. Hubbard and B. H. Flowers, Electron correlations in narrow energy bands, *Proceedings of the Royal Society of London. Series A. Mathematical and Physical Sciences* **276**, 238 (1963).
- [30] M. P. A. Fisher, P. B. Weichman, G. Grinstein, and D. S. Fisher, Boson localization and the superfluid-insulator transition, *Phys. Rev. B* **40**, 546 (1989).
- [31] D. Jaksch, C. Bruder, J. I. Cirac, C. W. Gardiner, and P. Zoller, Cold Bosonic Atoms in Optical Lattices, *Phys. Rev. Lett.* **81**, 3108 (1998).
- [32] E. Feenberg, *Theory of Quantum Fluids* (Academic Press, 1969).
- [33] E. H. Lieb and W. Liniger, Exact Analysis of an Interacting Bose Gas. I. The General Solution and the Ground State, *Phys. Rev.* **130**, 1605 (1963).
- [34] C. de Boor, *A Practical Guide to Splines* (Springer New York, 2001).
- [35] G. Roux, A. Minguzzi, and T. Roscilde, Dynamic structure factor of one-dimensional lattice bosons in a disordered potential: A spectral fingerprint of the Bose-glass phase, *New Journal of Physics* **15**, 055003 (2013).